Functional Damage Thresholds of Hafnia/Silica Coating Designs for the NIF Laser

Introduction

LLE's Optical Manufacturing Group (OMAN) has been tasked with coating several types of optics for use on the National Ignition Facility (NIF) laser system. Until recently, the standard quality assurance technique for coating large optics has been to process a smaller "witness" optic along with the large optic.Tests and inspections performed on the witness optic were used to certify the quality of the larger optic. This approach reduces costs and avoids damage to the production part. (The NIF optics used in this effort were 412 mm square. The corresponding witness optic would be 51 mm in diameter.)

One of the process factors that affects the durability of an optic is the cleanliness of the substrate prior to deposition of the thin-film, high-reflective coating. A particle on the substrate surface that is coated over creates a nodule that is much more likely to fail than any other portion of the coating. Current substrate cleaning and handling methods are so effective, however, that the number of particles per unit area present prior to coating is very small. As a result, the small-surface-area witness substrates have become statistically less likely to represent the damage properties of full-sized parts. For this reason, OMAN has been conducting a damage-testing experiment on its mirror coatings using full-sized NIF substrates. A large-area conditioning (LAC) station designed by LLNL was used for this testing.

The LAC station facilitates testing of full-sized samples by automatically scanning the test optic relative to an optical system that simultaneously irradiates a small area and detects any resulting damage. Repeated scans at increasing fluence were used to quantify the performance of candidate coating designs.

Three candidate high-reflector, thin-film coating designs using hafnia and silica were developed for the LM7E mirrors on the NIF laser. Mirrors were prepared with each candidate and damage tested to provide data that NIF planners could use, along with spectrophotometric results, to determine which coating design would work best for the NIF laser.

Objectives and Scope

Coating durability is the main issue investigated in this experiment. The coatings must be durable enough to survive the maximum fluence of the NIF's main beam (fluence being beam pulse energy per square centimeter). The reflectance/transmittance properties at other wavelengths are a secondary issue because the NIF plans to use alignment lasers that will operate on a different wavelength than that of the main beam. The selection of that wavelength can be based on the coating designs of the various optics in the system. Because variations in the coating designs may have positive or negative impact on damage thresholds, the optic's spectral performance and damage threshold are linked. The objective of this experiment is to find the best combination of coating durability and overall spectral performance for the NIF laser.

LLNL's definition of damage is "Functional Damage Threshold (FDT) is the minimum fluence at which a damaged optic degrades the performance of the NIF laser."† This represents a departure from traditional damage testing. Using this criterion meant that our first objective was to create some form of damage, and our second objective was to find the practical limit at which the optic could continue to function with that damage present. When the FDT is found, the resulting damage is termed "failure damage." Once failure damage has occurred, that damage site is likely to grow at fluences lower than the FDT. Figure 88.8(a) shows a damage site that has not reached its FDT; Fig. 88.8(b) shows a damage site that has reached its FDT.

If testing is continued on a failure damage site at the FDT fluence, that site will grow very rapidly. However, if the fluence is decreased from the FDT, the rate at which the site grows will decrease correspondingly. The growth threshold fluence (GTF) is the lowest fluence at which a site will continue to grow after it has sustained failure damage. Below the GTF, the size of the failure damage site will remain stable.

†This definition came from a presentation by C. Stolz at LLE regarding NIF definitions of damage.

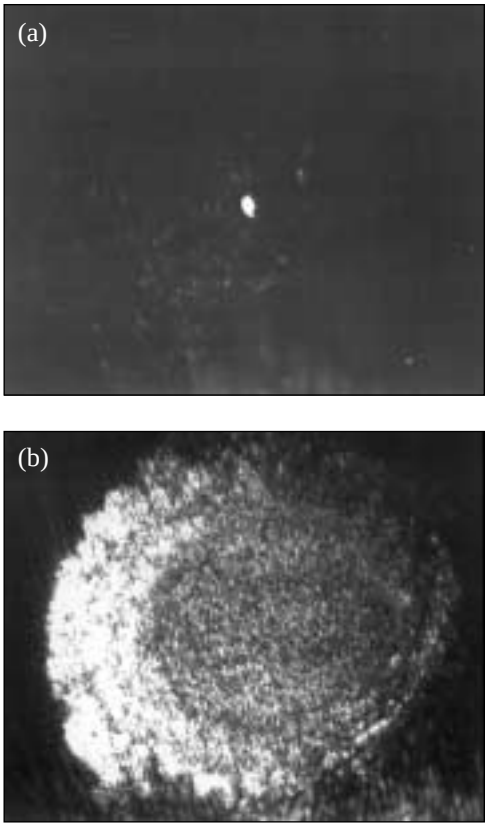

G5403

Figure 88.8
(a) A stable damage site ~0.13 mm in diameter. (b) The same site, after reaching it's FDT. During a single miniscan it grew to ~2.3 mm in diameter.

At the GTF, growth occurs at the lowest rate that can be positively detected. The GTF is always lower than the FDT.

During the course of the experiment, it was observed that the rate at which a damaged site grows after reaching the FDT is a function of the fluence used. At the GTF, the damage site is growing slowly enough that its size can be accurately measured. At fluences above the GTF, this becomes more difficult since the damage size quickly grows larger than available equipment can accurately measure. In order to obtain data for large numbers of shots, growth-rate testing was done at the GTF.

In summary, if the FDT, GTF, and the growth rate at the GTF are known, the fluence range over which the optic can perform without being damaged is also known. In addition, should that optic experience failure damage, the resulting operating limits can be estimated. These data can be used along with spectrophotometric results as criteria to select a coating design that is most suitable for the NIF optics.

Coatings

Three coating design options were tested on BK-7 substrates against a requirement of $Rs_{1054\ nm} > 99.5\%$ at 42.2° incidence. The NIF will be aligned with a UV laser, with a wavelength between 351 nm and 405 nm. (In this section, $Rs_{wavelength}$ stands for the reflectance in *s*-polarization at the wavelength in the subscript.) The different LLE coating designs try to maximize reflection about 351, 374, or 405 nm while maintaining the 1054-nm specification. They were named the Type-I, -II and -III coatings, respectively.

Types I and II used 22 alternating layers of HfO_2 and SiO_2 to form a first-order stopband reflector at 1054 nm. The refractive indices at 1054 nm are 1.993 for hafnia and 1.456 for silica. This resulted in physical thicknesses of 140.4 nm and 203.9 nm for the Type-I, high- and low-index quarter waves, respectively.

The Type-I and Type-II designs differed in that the stopband of Type II was shifted to 1078 nm, enabling the third-order reflectance $Rs_{374\ nm}$ to be >94%. In this design, the reflectance at 1054 nm is still above the specification but a slightly higher E-field is allowed to stand at the substrate/coating interface. Optimally a coating has E-field peaks occurring within a given layer of coating material instead of at an interface since the interface is structurally the weaker of the two. The spectral characteristics of the two types of coatings are shown in Fig. 88.9.

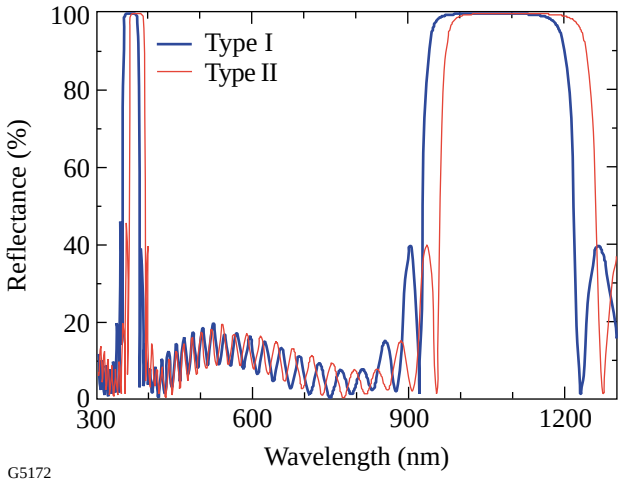

G5172

Figure 88.9
Reflectance versus wavelength for Type-I and -II coatings. The Type-II design at 42° incidence has a third-order stopband at 374 nm versus 351 nm for Type I.

The Type-III design is a computer-optimized, 32-layer design, with all layers of non-quarter-wave thickness. This was necessary to obtain $Rs_{351\ nm} < 7\%$ and $Rs_{405\ nm} > 94\%$ while maintaining $Rs_{1054\ nm} > 99.5\%$. Figure 88.10 shows the spectral characteristics of the Type-III design.

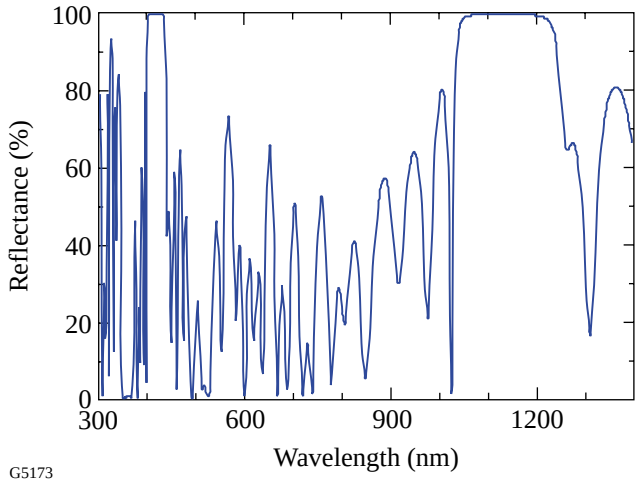

Figure 88.10
Reflectance versus wavelength for Type-III coating. The Type-III design is a non-quarter-wave design achieving high reflectance at 1054 nm and 405 nm while transmitting 351 nm at 42° incidence.

The coatings were deposited using electron-beam sources placed 120 cm below the planetary substrate plane. Hafnia layers were deposited at 0.16 nm/s by the evaporation of pure hafnium metal using a 7.5-kV electron-beam gun. This provided a consistent spit-free vapor in a 1×10^{-4}-Torr oxygen environment. Silica layers were deposited at 0.44 nm/s in 5×10^{-5} Torr of oxygen using an electron-beam gun at 6.0 kV. Achieving the correct oxygen pressure during silica deposition is important in balancing stresses for the two materials in their operating environment, which is air controlled to 40% relative humidity.

Experiment

The experiment was conducted using the LLNL-designed LAC station. The LAC station is capable of automating the entire damage testing and damage site detection process with a minimum of operator input. It consists of a precision *x*–*y* translation stage (shown in Fig. 88.11) that supports and positions the optic being processed, a fixed optical system for optic monitoring, a laser table that delivers the damage-testing beam and monitors beam characteristics, and a computer controller that operates the system and logs data sets.

Figure 88.11
The LAC station monitors an optic's surface quality at the same time it is being damage tested. The translation stage shown here can handle a variety of NIF optics, such as a NIF polarizer, which is 810 × 420 mm. Pictured on the stage is an LM2 substrate, approximately 420 × 420 mm.

The optical system that monitors the test optic is mounted in a fixed position in front of the translation stage (see Fig. 88.12). It is aligned so that the point at which its optical path intersects the front surface of the optic is the same point at which the damage-testing beam strikes the optic and is reflected away into a beam dump. This system uses a 633-nm diode laser to monitor scatter. A small reflector, mounted to the front of the telescope, reflects the diode's beam toward the

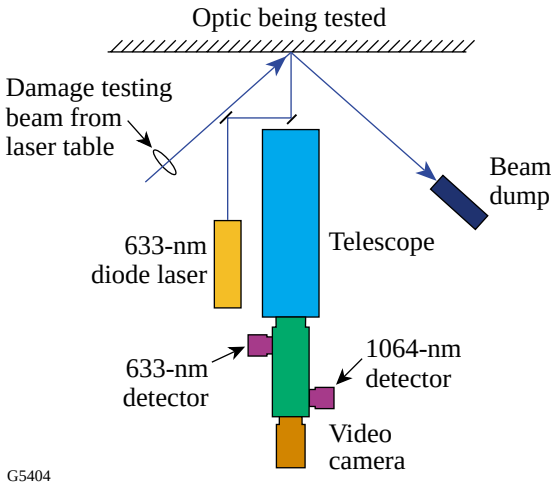

Figure 88.12
Optic monitoring system.

optic. If there is no scatter, i.e., the optic surface is undamaged, the diode beam will reflect back into this small reflector. If there is scatter, light will miss the reflector and be collected by the telescope. A 633-nm detector mounted to the back of the telescope collects the scatter data and relays it to the computer, which produces a scatter map of the optic.

In addition to the 633-nm detector, there is also a 1064-nm detector. Should the damage-testing beam strike the optic's surface and cause damage, 1064-nm light will scatter instead of reflecting into the beam dump. This scattered light is collected by the telescope and seen by the 1064-nm detector, which relays that data to the computer, which, in turn, produces what is called a "plasma map." A video camera completes the system; its output is sent to a video monitor and to the computer controller. The computer uses this input to capture digital still images when requested by the operator.

The laser table (shown in Fig. 88.13) includes the damage-testing laser (characteristics discussed below), a camera, and a power meter. The camera monitors the beam's cross section, while energy levels are measured via the power meter head. Both sets of data are relayed to the LAC computer program, which calculates the geometric characteristics of the beam based on the camera data and then combines it with the measured energy levels to determine the instantaneous and average fluence of the beam. All of these results are logged by the program.

An OMAN addition to the LAC system was a digital video recorder. The signal was taken from the line connecting the video monitor to the computer. The recorder was used to document the actual damage as it occurred when a miniscan was performed (miniscans are defined below).

The experiment was conducted using the LAC in a class-1000 clean-room environment at LLE as follows: Damage tests were performed by raster-scanning a *Q*-switched Spectra Physics Quanta-Ray Pro Nd:YAG laser emitting 1064-nm light with a 30-Hz repetition rate and a 10-ns pulse length. Beam characteristics (energy/shot and beam cross section) were sent directly from the data acquisition hardware to the LAC program. The program automated all pertinent calculations and controlled the substrate position with respect to the laser beam. The program scales the fluences it reports to a 3-ns pulse length, using the following experimentally derived scaling equation:

$$F_x = F_y(x/y)^{0.35}, \tag{1}$$

where x and y are the two pulse lengths of interest and $F_{x \text{ or } y}$ is the fluence at that pulse length.

During the procedure described below, the clear aperture of the optic was divided into two halves: one half was reserved for *s*-polarization testing, the other for *p*-polarization. Damage testing was performed on one half of the optic at a time.

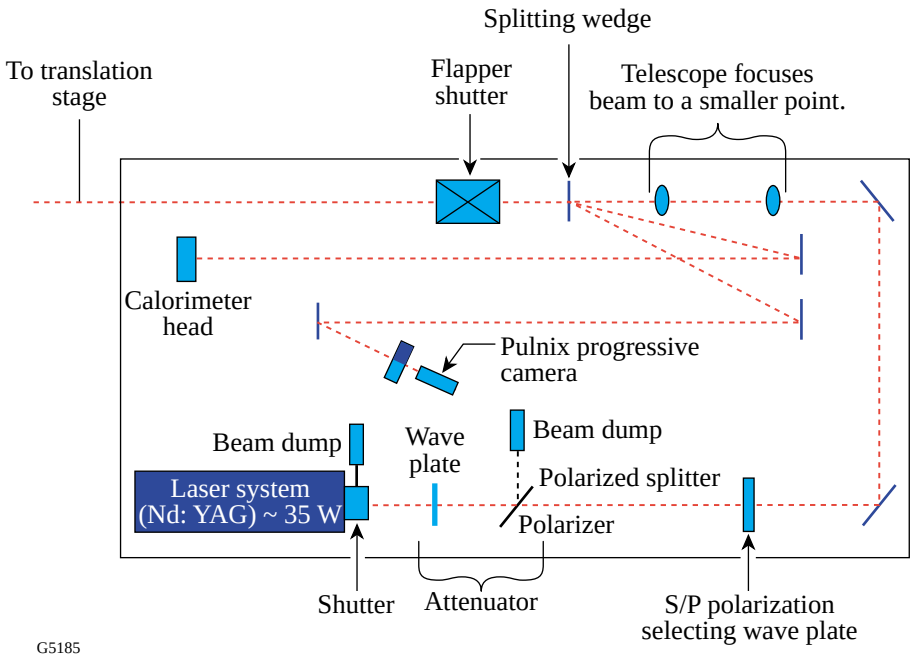

Figure 88.13
Schematic of the LAC laser table layout. The length of the beam path between the splitting wedge and camera is equal to that between the splitting wedge and testing plane.

A full scan was performed first on the half of the aperture being tested. The fluences (scaled to a 3-ns pulse) used for these scans were 15, 18, 22, 25, 30, and 35 J/cm^2. After each full scan was completed (approximately 6 h), the scatter map of the optic's surface was examined for possible defect sites. The optic was also examined by eye for possible defect sites.

Once a defect site (or potential defect site) was found, it was made the center of a "miniscan." A miniscan is a 10-mm-wide by 5-mm-tall raster scan, with the candidate defect site at the center. A scatter site was said to be "stable" at a given fluence if no growth occurred after three sets of five miniscans (15 miniscans total) were done on the site. If the site was determined to be stable, another full scan was done at the next-highest fluence. The miniscan process was then repeated at that fluence. This fullscan/miniscan process was repeated until the damage site became unstable.

Once a scatter site was found to be unstable (damage growth occurred prior to the 15th miniscan), the fluence causing the damage growth was recorded as the FDT and determination of the GTF was started.

The procedure used to determine the GTF is the same as that used to determine the FDT, with two exceptions: (1) no full scan is performed, and (2) the first miniscan fluence is 12 J/cm^2 instead of 15 J/cm^2 (the scaled-to-3-ns-fluence steps are 12, 15, 18, 22, and 25 J/cm^2). The same criteria that determined the FDT also apply to the GTF (three sets of five miniscans). If the damage site was found to be stable at 12 J/cm^2, the fluence was increased and the procedure repeated.

Data Gathering

Multiple damage sites were examined on each of the Type-I, -II, and -III optics. A photothermal printer was used to produce images of identified damage sites prior to and after each full scan and group of miniscans. These images were then measured with a circle template and scaled to the appropriate dimensions. It should be noted that one constraint of this method is that only the lateral size of defects, not changes in depth, can be measured; therefore, throughout this experiment, damage growth refers only to a change in dimension tangent to the surface of the optic.

The fluence at which a scan, or group of scans, was performed was also recorded, as well as how many of those scans were performed. These three parameters—lateral defect size, scan fluence, number of scans—were then used for analysis.

Data Analysis

The average growth rate can be determined if an extended number of shots are taken at the GTF. Two sites were tested in excess of 50 raster scans at the GTF. A definite trend in the growth of the damage size could be seen when it was plotted as a function of the number of raster scans. A trend line was fit to the data points, the slope of which is the change in size as a function of raster scans, or the average growth rate.

Figure 88.14 is a plot of the data collected at the GTF at two sites. As is evident, the growth rates of these two sites are nearly identical (roughly 14.0 and 14.4 μm/miniscan) through the course of approximately 120 miniscans.

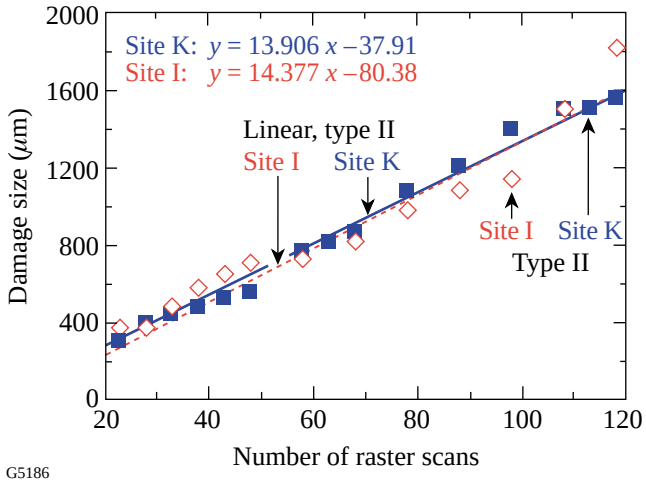

Figure 88.14
Plot of damage size versus number of raster scans at a fluence of 22.5 J/cm^2 for 10-ns pulses.

Results and Conclusion

The results for the Type-I, -II, and -III coated LM7E's are listed in Table 88.I. Each fluence listed is the lowest for its particular category and is scaled from the 3-ns-pulse-length number reported by the LAC program to its 10-ns counterpart. The FDT numbers represent the lowest damage thresholds found on a particular coating design/polarization. For each coating design/polarization combination, a minimum of ten damage sites were investigated.

The following conclusions can be drawn:

1. The damage thresholds of the Type-I coatings were greater than those of the Type-II or -III coatings.
2. The GTF was the same for all three coating designs.

Due in part to the results of this experiment, the NIF project has decided to go with a slightly modified version of the Type-II coating. This "Type-IV" coating differs from the Type II in that the top and bottom three layers of the coating stack are modified. This was done for two reasons. The first is to improve performance over the Type-II design. The second has to do with an additional requirement (not addressed by this experiment) regarding backscattered stimulated Brillion scattering (SBS) and 400- to 700-nm stimulated Raman scattering (SRS) light from the target chamber. Spectral measurements performed by LLNL show the Type-IV design more effectively suppresses SBS and SRS than the Type-II design.

ACKNOWLEDGMENT

This work was supported by the U.S. Department of Energy Office of Inertial Confinement Fusion under Cooperative Agreement No. DE-FC03-92SF19460, the University of Rochester, and Lawrence Livermore National Laboratories under subcontract B399901. The support of DOE does not constitute an endorsement by DOE of the views expressed in this article.

Table 88.I: FDT's and GTF's for the three LM7E mirror designs.

(All 10 ns in J/cm^2)	*p*-pol FDT	*s*-pol FDT	*p*-pol GTF	*s*-pol GTF
Type I	37	42	22	22
Type II	37	33	22	22
Type III	33	33	22	22
The precision of the listed fluences is ±3 J/cm^2.				